Biomedicine & Pharmacotherapy 67 (2013) 221–227

Available online at
SciVerse ScienceDirect
www.sciencedirect.com

Elsevier Masson France
EM|consulte
www.em-consulte.com/en

Original article

The roles of macromolecules in imatinib resistance of chronic myeloid leukemia cells by Fourier transform infrared spectroscopy

Yusuf Baran [a,*], Cagatay Ceylan [b,**], Aylin Camgoz [a]

[a] İzmir Institute of Technology, Department of Molecular Biology and Genetics, Urla, 35430 İzmir, Turkey
[b] İzmir Institute of Technology, Department of Food Engineering, Urla, 35430 İzmir, Turkey

ARTICLE INFO

Article history:
Received 19 November 2012
Accepted 7 December 2012

Keywords:
Imatinib
Chronic myeloid leukemia
Multidrug resistance
Fourier transform infrared spectroscopy

ABSTRACT

Imatinib is a first generation tyrosine kinase inhibitor, which is used for the treatment of chronic myeloid leukemia. However, resistance to imatinib is an important problem. Different mechanisms have been explained for imatinib resistance. In this study, we examined the roles of macromolecules in imatinib resistance in K562 cells at the molecular level using Fourier Transform Infrared (FT-IR) spectroscopy. An amount of 3 μM imatinib resistant cells were generated by our group and named as K562/IMA-3 cells. Changes in macromolecules in parental and resistant cells were studied by FT-IR spectroscopy. Imatinib resistance caused changes, which indicated decreases in the level of glycogen and increases in the membrane order. The amount of unsaturated lipids increased in the imatinib resistant cells indicating lipid peroxidation. Imatinib resistance caused changes in the lipid/protein ratio. The relative protein content increased with respect to nucleic acids indicating higher transcription and protein expression and structural/organizational changes in the nucleus were evident as revealed by frequency changes in the nucleic acid bands. Changes in the amide bands revealed changes in the proteome of the resistant cells. Protein secondary structural changes indicated that the antiparallel beta sheet's structure increased, however the alpha helix structure, beta sheet structure, random coil structure and turns decreased in the resistant cells. These results indicate that the FT-IR technique provides a suitable method for analyzing drug resistance related structural changes in leukemia and other cancer types.

1. Introduction

Reciprocal translocation between chromosomes 22 and 9 generates BCR/ABL oncogene, which is the main cause of chronic myeloid leukemia. BCR/ABL inhibits differentiation and apoptosis and induces cell growth and proliferation. Imatinib is the first anticancer agent targeting BCR/ABL oncoprotein for the treatment of chronic myeloid leukemia (CML) patients. It binds to ATP binding site of BCR/ABL oncoprotein and inhibits its kinase activity that results in inhibition of leukemogenesis [1,2]. Although high rates of hematological and cytogenetical responses, resistance to imatinib is still the main problem for successful treatment of CML. Different mechanisms were explained for imatinib resistance, such as overexpression of BCR/ABL, changes in nucleotide sequence of ATP binding site of BCR/ABL, inhibition of apoptosis, aberrant ceramide metabolism and overexpression of transporter genes [3–6].

Fourier transform infrared spectroscopy is a method used to monitor molecular changes in the analysis of biological systems. The method allows for rapid, sensitive and non-destructive method analysis of samples in any physical state [7,8]. The spectral data can be analyzed with many different digital manipulations, producing both qualitative and quantitative information considering shifts in peak positions, changes in bandwidths and band intensities to obtain structural and functional information about the systems analyzed. The data can be used for detection of changes in cellular components such as lipids, proteins, carbohydrates and nucleic acids at the level and in close vicinity of functional groups simultaneously [7,9].

Since an FT-IR spectrum is a molecular fingerprint of the studied tissue or cells, the technique can be suitably used to follow the changes specific for biological differentiation processes such as disease processes during which metabolic changes with alterations in carbohydrate, lipid and protein profiles occur. Similarly, FT-IR technique has been developed to be a valuable diagnostic tool to analyze and detect changes at the molecular level in cancer [10,11].

In this study, we examined the possible roles of macromolecules in imatinib resistance by Fourier transform infrared spectroscopy (FT-IR). For this purpose, imatinib resistance was

* Corresponding author. Tel.: +90 232 7507515; fax: +90 232 7507509.
** Corresponding author. Tel.: +90 232 750 6328; fax: +90 232 750 6196.
E-mail addresses: yusufbaran@iyte.edu.tr (Y. Baran), cagatayceylan@iyte.edu.tr (C. Ceylan).

0753-3322/$ – see front matter © 2013 Elsevier Masson SAS. All rights reserved.
http://dx.doi.org/10.1016/j.biopha.2012.12.001

induced in K562 cells. Although resistance-dependent macromolecular changes in various types of cancers against different anticancer drugs including nilotinib have been investigated using FT-IR technique [12–14], this is the first detailed study investigating the changes between sensitive and 3 μM imatinib resistant K562/IMA-3 cells in terms of biochemical variations.

2. Materials and methods

2.1. Cell lines and culture conditions

K562 CML parental cells were obtained from the German collection of microorganisms and cell cultures (Germany). The cells were cultured in RPMI-1640 growth medium (Biological Industries, Israel) containing 15% fetal bovine serum (Biological Industries, Israel) and 1% penicillin-streptomycin (Biological Industries, Israel) at 37 °C in 5% CO_2. Medium was refreshed every 3 days. The cell suspension was taken from tissue culture flasks into a sterile falcon tube and was centrifuged for 10 min at 1000 rpm. The supernatant was removed and the pellet was washed with 2 ml of phosphate buffered saline (PBS). The cells were recentrifuged at 1000 rpm for 10 min. The cells were resuspended in 15 ml of RPMI-1640 medium and transferred into sterile culture flasks.

2.2. Sample preparation for FT-IR spectroscopy

We used 5×10^6 cells grown in 15 ml of RPMI-1640 medium. The cells were collected and dissolved in sterile distilled water. The collected cells were lyophilized in a freeze drier (Labconco, FreeZone 18 liter freeze dry system) overnight to remove water. The cell powder was mixed with dried potassium bromide (KBr) (Sigma-Aldrich, USA) in a mortar (at a ratio of 1:100). The mixture was then pressurized to 100 kg/cm^2 (1200 psi) for 5 min. All the cell growth, cell collection and FT-IR experiments for the imatinib sensitive and resistant K562 cells were carried out on the same day.

2.3. FT-IR spectrum accumulation and data processing

The spectral analysis was carried out using a PerkinElmer spectrometer equipped with MIR TGS detector (Spectrum 100 Instrument, PerkinElmer Inc., Norwalk, CT, USA). FT-IR spectra of the samples were recorded between 4000 and 450 cm^{-1}. Interferograms were averaged for 20 scans at 4 cm^{-1} resolution. The background spectrum was automatically subtracted from the spectra of the samples. Spectrum 100 software (PerkinElmer) was used for all data manipulations.

From each sample, at least three different scans, which gave identical spectra, were performed. These replicates (n = 7 for the sensitive; n = 12 for the resistant cells) were averaged and the averaged spectra for each sample were then used for further data manipulation and statistical analysis. The spectra were smoothed over 19 points using the Savitzky–Golay algorithm. Then, the spectra were interactively baselined from two arbitrarily selected points. Finally, the spectra were normalized in specific regions for visual comparison of the imatinib sensitive and resistant samples.

For determination of protein secondary structural changes, the second derivative spectra were obtained by applying a Savitzky–Golay algorithm with five points. The second derivatives were normalized between 1700 and 1600 cm^{-1} and the peak intensities were calculated. The peak minima of the second derivative signals were considered because they correspond to the peak minima of the original absorption spectra [15].

2.4. Statistical analysis

The differences between the imatinib-sensitive and resistant groups were compared using the Mann–Whitney U Test with the Matlab R2011a program. The statistical results are expressed as means ± standard deviation. $P < 0.05$ was considered statistically significant.

3. Results

3.1. FT-IR studies

We previously reported that IC50 values of imatinib for K562 and K562/IMA-50 cells were found to be 280 and 14680 nM, respectively. However, the results revealed that K562/IMA-3 cells were much more resistant to imatinib as compared to K562 cells [15].

The FT-IR spectroscopy technique is a technique, which investigates biological systems at the molecular level and provides information about the structure [7] and function of the macromolecular constituents such as lipids, proteins and nucleic acids [9]. Hence, the technique was used in the analysis of the effects of imatinib resistance on K562 cells in our studies.

Fig. 1 shows the average FT-IR spectra of control K562 cells in the 3660–940 cm^{-1} spectral region. Assignments of the major bands in Fig. 1 are presented in Table 1. The FT-IR spectrum of K562 cells consists of several bands originating from the contribution of different functional groups of macromolecules. The spectra were analyzed for the following regions: 2820–3660 cm^{-1} for the analysis of proteins and lipids, and 1595–1775 cm^{-1} for the analysis of proteins and lipids, 940–1480 cm^{-1} for the analysis of the fingerprint region. All the spectra presented in the figures were normalized with respect to specific selected bands and were used only for illustrative purposes. However, in the measurement of the spectral parameters, each original baseline-corrected spectrum belonging to the corresponding control and treated groups was considered separately.

3.2. 2820–3660 cm^{-1} region

The average FT-IR spectra of the sensitive and K562/IMA-3 cells in the 2820–3660 cm^{-1} spectral region is shown in Fig. 2. The FT-IR spectrum in this region consists of amide A and amide B bands which have contributions from mainly the N–H stretching of proteins with a small contribution from the O–H stretching of polysaccharides and intermolecular H bonding and contributions from C–N and N–H stretching of proteins, respectively. In addition, the olefinic =CH stretching vibration band located around 3011 cm^{-1}, which has contributions from cholesterol esters

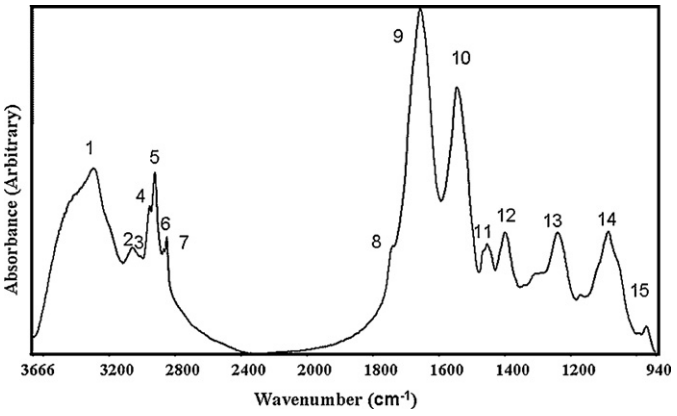

Fig. 1. The general FT-IR spectrum of K562 cells in 3660–940 cm^{-1} region.

Table 1
The general FT-IR band assignments of K562 cells.

Band number	Wave numbers (cm^{-1})	Definition of the spectral assignment
1	3300	Amide A: mainly N–H stretching of proteins with the little contribution from O–H stretching of polysaccharides and intermolecular bonding
2	3061	Amide B: C–N and N–H stretching of proteins
3	3011	Olefinic =CH stretching vibration: unsaturated lipids, cholesteryl esters
4	2959	CH_3 asymmetric stretching: lipids, protein side chains, with some contribution from proteins, carbohydrates
5	2925	CH_2 asymmetric stretching: mainly lipids, and the little contribution from proteins and carbohydrates
6	2873	CH_3 symmetric stretching: protein side chains, lipids and with some contribution from carbohydrates and nucleic acids.
7	2854	CH_2 symmetric stretching: mainly lipids, with the little contribution from proteins, nucleic acids and carbohydrates
8	1743	Ester C=O stretching: triglycerides and cholesterol esters
9	1657	Amide I: proteins, mainly C=O stretch
10	1546	Amide II: proteins, mainly N–H bend and C–N stretch
11	1452	CH_2 bending: mainly lipids, with the little contribution from proteins, CH_3 asymmetric bending: methyl groups of proteins
12	1399	COO– symmetric stretch: mainly lipids with the little contribution from proteins; CH_3 symmetric bending: methyl groups of proteins
13	1239	PO_2^- asymmetric stretch: mainly nucleic acids with the little contribution from phospholipids
14	1086	PO_2^- symmetric stretch: nucleic acids and phospholipids; C–O stretch: glycogen
15	971	C–N+–C stretch: nucleic acids

[16]. The CH_3 asymmetric stretching band located at 2959 cm^{-1} has contributions from both lipids and proteins; the CH_2 asymmetric stretching band located at 2925 cm^{-1} is mainly due to lipids; the CH_3 symmetric stretching band located at 2873 cm^{-1} is mainly due to protein side chains with some contribution from lipids, carbohydrates and nucleic acids and CH_2 symmetric stretching band located at 2854 cm^{-1} monitors mainly lipids, with small contributions from proteins, nucleic acids and carbohydrates [8,17].

Imatinib resistance induced remarkable changes in the bandwidth, intensity and frequency value of the FT-IR bands in this region as seen from Fig. 2. Comparisons of the band intensities of some infrared bands of imatinib sensitive and resistant K562 cells are shown in Fig. 3. As can be seen from Fig. 2, there was a reduction in the intensity of amide A band which is located at 3300 cm^{-1}, however the intensity of the amide B band which is located at 3061 cm^{-1} was increased amide B band contains strong absorptions arising mainly from C–N and N–H stretching of proteins mode of proteins and of K562 cells. When normalized with the intensity of the amide I band, 9.80% reduction was observed for imatinib resistant cells for amide A band as seen in Fig. 3. The frequency of the amide A band shifted from 3300.12 ± 0.720 to 3300.443 ± 0.351 cm^{-1} in K562/IMA-3 cells only slightly ($P = 0.5826$). However, the frequency of the amide B band shifted from 3061.315 ± 1.084 to 3061.444 ± 1.274 cm^{-1} in imatinib resistant K562 cells [16,18–20].

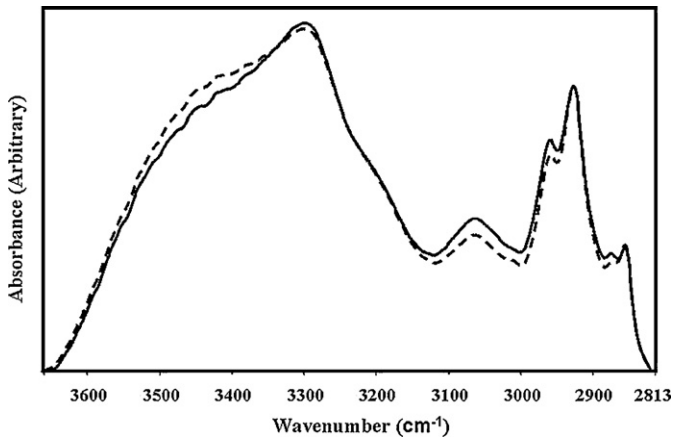

Fig. 2. The FT-IR spectra of imatinib sensitive (solid line) and resistant (dotted line) cells in the 3660–2820 cm^{-1} region (the spectra were normalized with respect to CH_2 asymmetric mode, which is observed at 2925 cm^{-1}).

The absorptions arising from C–H stretching vibrations of aliphatic compounds is populated between 3000 cm^{-1} and 2820 cm^{-1} as shown in Fig. 4. When normalized to the band at 2925 cm^{-1}, the intensity of the CH_3 asymmetric band at 2959 cm^{-1} and CH_3 symmetric stretch band at 2872 cm^{-1} decreased for K562/IMA-3 cells, whereas the intensity of the CH_2 symmetric stretch band at 2854 cm^{-1} increased slightly for K562/IMA-3 cells. In Fig. 3 the intensity ratio of 2874 cm^{-1} and 2852 cm^{-1} decreased by 5.043% in K562/IMA-3 cells ($P < 0.0001$). The frequency of the CH_3 asymmetric stretch band around 2959 cm^{-1} band shifted from 2959.213 ± 0.136 to 2958.680 ± 0.105 cm^{-1} ($P < 0.005$) and the frequency of CH_3 symmetric stretching band located around 2873 cm^{-1} shifted from 2873.255 ± 0.078 to 2872.435 ± 0.056 ($P < 0.005$) in K562/IMA-3 cells.

The intensity of the band at 3011 cm^{-1} increased 4.82 fold in K562/IMA-3 cells. Since this band is due to the CH stretching of HC=CH groups, it can be said that the degree of unsaturation increases in the imatinib resistant cells.

3.3. 1595–1775 cm^{-1} region

The average FT-IR spectra of the sensitive and K562/IMA-3 cells in the 1775–1595 cm^{-1} spectral region is shown in Fig. 5. The band centered at 1743 cm^{-1} is mainly assigned to the C=O ester stretching vibration of triglycerides and cholesterol esters [7,21,22]. As seen in Fig. 5, the intensity and frequency of the C=O ester stretching vibration increased for K562/IMA-3 cells. The bands at 1657 cm^{-1} and 1546 cm^{-1} are amide I and amide II bands of proteins. Both of them are known to be sensitive to protein conformation and are used to determine the secondary structure content of proteins. Changes in the shapes of these two bands indicated changes in the proteomes of the imatinib resistant cells. In Fig. 3 the ratio of the intensities of Amide I/Amide II bands increased (3.65%) for K562/IMA-3 cells [7].

In addition, the secondary derivative of the Amid I band showed changes in the alpha helix band around 1656 cm^{-1} and loss of random coil band around 1648 cm^{-1} for K562/IMA-3 cells as seen in Fig. 6 The assignments of the secondary structural components and the intensities of the sub-bands are given in Tables 2 and 3, respectively. The results revealed that the antiparallel beta sheet structure increased slightly, however, the alpha helical structure (located at 1653 cm^{-1}), random coil structure (located at

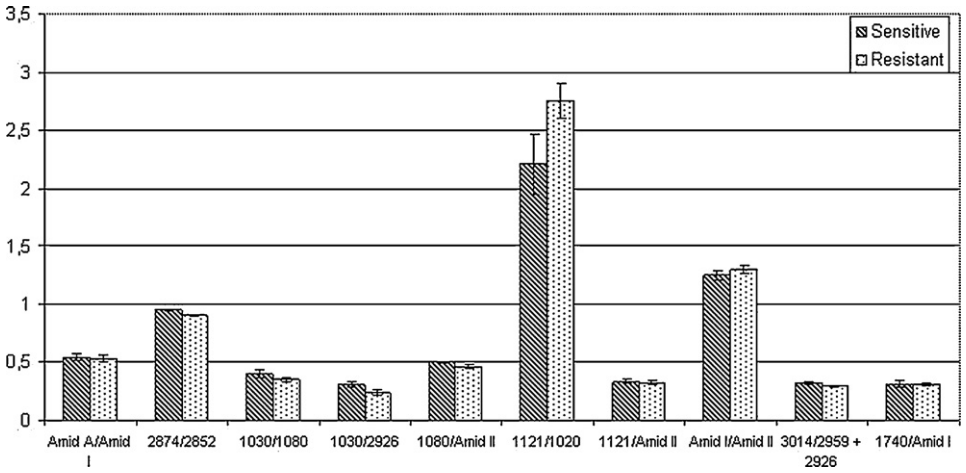

Fig. 3. The intensity-ratio values of the bands for imatinib sensitive and resistant K562 cells. The values are the mean ± standard deviation for each group.

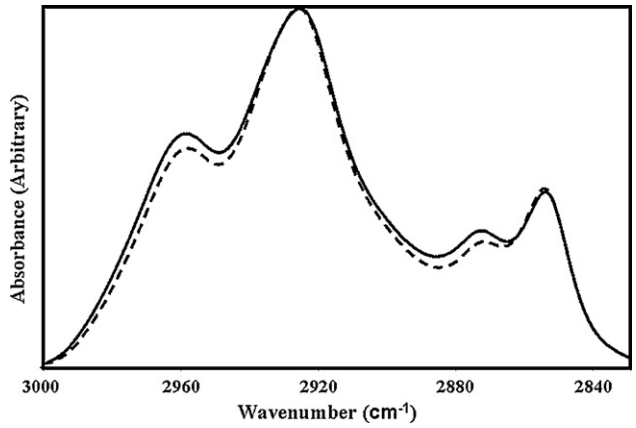

Fig. 4. The FT-IR spectra of imatinib sensitive (solid line) and resistant (dotted line) cells in the 3000–2820 cm^{-1} region (the spectra were normalized with respect to CH_2 asymmetric mode, which is observed at 2925 cm^{-1}).

1648 cm^{-1}), the beta sheet structure (located at 1637 cm^{-1}) and the turns (located at 1674 cm^{-}1) decreased slightly in the imatinib resistant cells ($P < 0{,}05$).

3.4. 940–1480 cm^{-1} (fingerprint) region

The average FT-IR spectra of the imatinib sensitive and resistant K562 cells in the 940–1480 cm^{-1} spectral region is shown in Fig. 7A–C. The band at 1452 cm^{-1} is attributed to CH_2 bending vibration of lipids [23,24]. The frequency of the band around 1453 cm^{-1} shifted from 1452.951 ± 0.451 to 1454.56 ± 0.266 cm^{-1} in K562/IMA-3 cells as seen in Fig. 7A ($P < 0.005$). The band at 1399 cm^{-1} is attributed to COO^{-} symmetric stretch of mainly lipids with a small contribution from proteins (Jackson et al., 1998) The frequency of the band around 1399 cm^{-1} shifted from 1399.503 ± 0,319 to 1400 ± 0.311 cm^{-1} ($P < 0.005$). The bands at 1239 and 1086 cm^{-1} are of nucleic acids and attributed to PO_2^{-} asymmetric and symmetric stretch [25,26]. The frequency of the band around 1085 cm^{-1} band shifted from 1086.00 ± 0.338 to 1086.637 ± 0.037 cm^{-1} in K562/IMA-3 cells ($P < 0.005$) as in Fig. 7C. The band at 1155 cm^{-1} is attributed to C–O stretching of glycogen [27]. A notable decrease in the intensity of this band was observed in the K562/IMA-3 cells as seen in Fig. 7B. The band at 970 cm^{-1} is assigned to C–N^{+}–C stretch of nucleic acids [28].

In the analysis of the bands in this region the intensity ratio of the 1030 cm^{-1} and 1080 cm^{-1} bands decreased by 12.90% in K562/IMA-3 cells ($P < 0.005$) as seen in Fig. 3. Similarly, in the same figure the intensity ratio of 1030 cm^{-1} and 2926 cm^{-1} bands decreased by 22.04% ($P < 0.005$); 1080 cm^{-1} and Amide II bands increased by 2.78% ($P < 0.005$) and 1121 cm^{-1} and Amide II bands decreased by 4.08% ($P = 0.1391$) in K562/IMA-3 cells. However, a considerable increase (19.79%) in the intensity ratio of the 1121 cm^{-1} and 1020 cm^{-1} bands was observed in K562/IMA-3 cells ($P < 0.005$) as seen in Fig. 3.

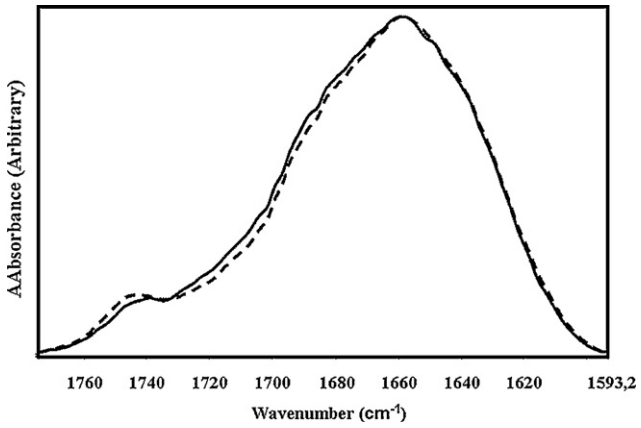

Fig. 5. The FT-IR spectra of imatinib sensitive (solid line) and resistant (dotted line) cells in the 1775–1595 cm^{-1} region (the spectra were normalized with respect to amide I band, which is observed at 1657 cm^{-1}).

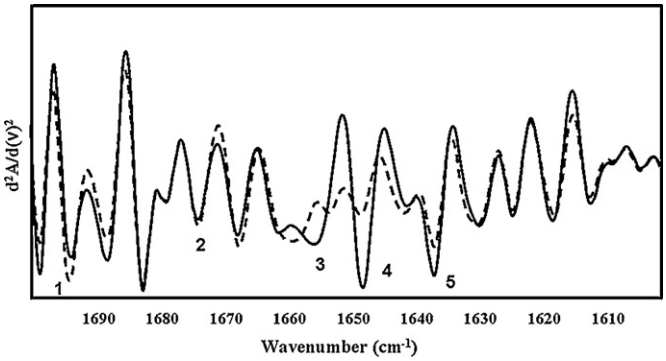

Fig. 6. The average second derivative spectra of imatinib sensitive (solid line) and resistant (dotted line) K562 cells in 1700–1600 cm^{-1} region.

Table 2
The assignments of secondary structure sub-bands under amide I band in 1700–1600 cm^{-1} region for imatinib sensitive and resistant K562 cells [15].

Peak number	Mean frequencies (cm–1)	Assignment
1	1694	Antiparallel beta sheet
2	1674	Turns
3	1653	Alpha helix
4	1648	Random coil
5	1637	Beta sheet

4. Discussion

Targeting the tyrosine kinase activity of BCR-ABL is a common and attractive therapeutic strategy for effective treatment of chronic myeloid leukemia. Imatinib is a very effective tyrosine kinase inhibitor, which gives positive results in first line treatment of CML patients. Unfortunately, CML cells can somehow escape from the apoptotic effects of imatinib and acquire resistance. This is the most important problem in the clinic to get successful results. The molecular mechanisms of multidrug resistance in CML were shown by our group and other researchers [3,4,29]. However, changes in macromolecular levels in imatinib resistant CML cells and the roles of these differences on imatinib resistance were not examined and discussed in the literature. In this study, we investigated the changes in macromolecular structures in imatinib resistant CML cells by using FT-IR and compared the results with the sensitive cells.

In the preparation of the samples, water was removed from the samples in the sample preparation steps using lyophilization procedures in this study. Hence, contribution from water to Amid A, Amid B, Amid I and Amid II bands was negligible. For this reason, the 3300 cm^{-1} band can be considered to be due to only proteins and polysaccharides. The reduction in the intensity ratios of Amid A to Amid I in the imatinib resistant cells can be due to the reduced contribution of glycogen since a decrease was observed in the intensity of the 1155 cm^{-1} band which is mainly assigned to the C–O stretching vibrations of glycogen [27]. Since cancer cells are known to consume more carbohydrate due to their increased energy expenditure which is known as the Warburg Effect. The reduction in the intensity of these two bands could be ascribed to reduce contribution of polysaccharides in the resistant cells [30]. Similarly, drug resistance is hypothesized to require more energy for the additional tasks of elimination of toxic compounds and drugs.

The intensity of the band at 3015 cm^{-1} which is due to CH stretching of olefinic HC=CH stretching vibrations indicates that the population of unsaturated lipids increased in the resistant cells. In addition, the increase in the olefinic band may be due to the accumulation of end products of lipid peroxidation and a change in phospholipid metabolism [31]. The increase in the level of unsaturation was found to be 4.82 times higher than that of the sensitive cells. It appears that drug resistant cells have better resistance to reactive oxygen species such as peroxides. This conclusion is supported by the results obtained from the bands around 1743 cm^{-1}. The change in shape and frequency of the band around 1743 cm^{-1} indicated the changes in the ratio of triglycerides and cholesterol esters and their saturation states, it is seen that in K562/IMA-3 cells, the maximum of the band shifts to higher frequency values and the intensity also increases at around 1743 cm^{-1} in Fig. 5 and it is known that packing of ester groups in the constituent fatty acids is strongly dependent on their saturation state.

The decrease in CH_3 asymmetric stretching vibration absorption intensity in the imatinib resistant cells indicates a change in the composition of the acyl chains in lipids as shown in Fig. 2 [32].

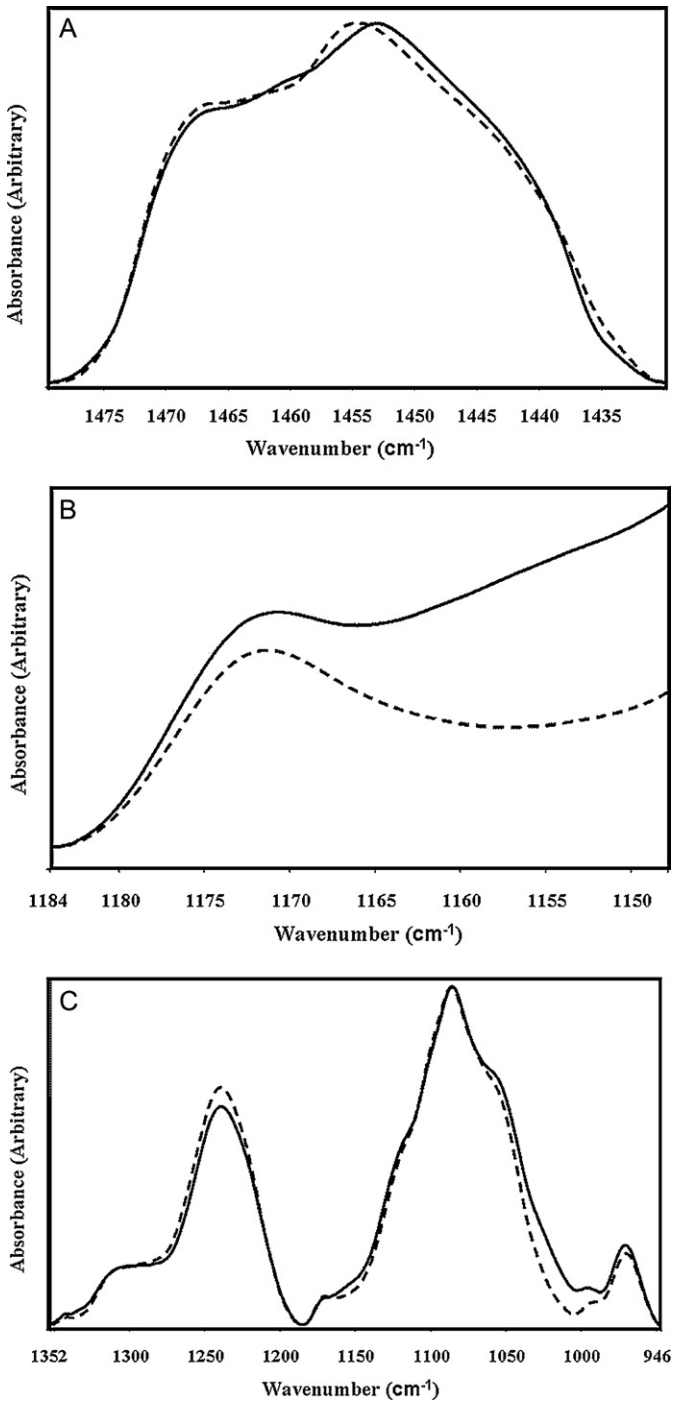

Fig. 7. The FT-IR spectra of imatinib sensitive (solid line) and resistant (dotted line) cells (a) in the 1480–1430 cm^{-1} region (the spectra were normalized with respect to CH_2 bending mode, which is observed at 1452 cm^{-1}); b: in the 1184–1145 cm^{-1} region; c: in the 1350–940 cm^{-1} region (the spectra were normalized with respect to PO_2^- symmetric stretching mode, which is observed at 1086 cm^{-1}).

In addition, the frequency of the CH_3 asymmetric stretch band shifted from 2959.213 to 2958.68 cm^{-1} in K562/IMA-3 cells. The decrease in the frequency corresponds to decreasing freedom of the acyl chain in the center of the bilayer since the CH_3 asymmetric stretching mode is correlated with the order of the deep interior of the membrane [17]. Hence, the order in the lipid plasma membrane interior is increased in the resistant cancer cells [33]. In addition, the intensity of the CH_2 symmetric stretching band decreased in the resistant cells indicating a decreasing proportion

Table 3
The results of the changes in the intensities of main protein secondary structures for imatinib sensitive and resistant K562 cells.

Functional groups	Sensitive	Resistant	*P* values
Antiparallel beta sheet structure (located at 1694 cm^{-1})	−0.01249 ± 0.00135	−0.0133 ± 0.00301	$P < 0,05$
Turns (located at 1674 cm^{-1})	−0.01027 ± 0.002127	−0.00945 ± 0.002147	$P < 0,05$
Alpha helical structure (located at 1653 cm^{-1})	−0.0134 ± 0.01082	−0.01082 ± 0.002363	$P < 0,05$
Random coil structure (located at 1648 cm^{-1})	−0.01487 ± 0.002246	−0.00915 ± 0.002431	$P < 0,05$
Beta sheet structure (located at 1637 cm^{-1})	−0.01371 ± 0.002187	−0.01045 ± 0.00098	$P < 0,05$

of the CH_2 groups in the resistant cells. Similarly, the frequency of the bending vibration at 1452 cm^{-1} shifted from 1452.95 to 1454.56 cm^{-1} in K562/IMA-3 cells indicating changes in the lateral packing property of the methylene groups in the membrane lipids [34].

A precise protein-to-lipid ratio can be derived by calculating the intensity ratio of the CH_3 symmetric stretching (2874 cm^{-1}) to the CH_2 symmetric stretching vibration (2852 cm^{-1}) from the FT-IR spectra [7]. The intensity ratio of 2874 cm^{-1} and 2852 cm^{-1} was found to decrease by 5.04% in K562/IMA-3 cells. These results indicate an increase in the lipid content of the cellular material for constant protein content. Although there have been contrasting reports of the change in the amount of lipids in drug resistant cells, in general lipidation is considered to be one of the general response of the cell to toxic environments [35,36].

Amide I band frequency and shape is sensitive to protein conformation. The changes in the shape of the Amide I band as seen in Fig. 5 are attributed to the changes in protein conformation [37]. In addition, the intensity ratio of Amide I/Amide II was found to increase 3.80% for K562/IMA-3 cells indicating protein secondary structural changes. Although this ratio was ascribed to the changes in only membrane proteins by Zhou et al. in HL60 cells that underwent apoptosis, in this study it describes a total change in the proteome and protein structural changes of that proteome [38]. Protein kinase inhibitors can change the cellular metabolism considerably. As toxic drugs they can initiate endoplasmic reticulum stress response via the expression of proteins such as chaperones and heat shock proteins to alleviate the adverse effects [39]. The proteome of the resistant cells change as a result. In another study investigating doxorubicin resistance observed an increase in the band around 1690 cm^{-1} (antiparallel beta sheets) similar to our results [13].

The nucleic acid bands appear at 1239 cm^{-1}, 1086 cm^{-1} and 971 cm^{-1}. The 1239 cm^{-1} band is due to asymmetric phosphate stretching and the 1086 cm^{-1} band is due to symmetric phosphate stretching band of nucleic acids [25,26]. The band at 970 cm^{-1} is due to C-N^+-C stretching of nucleic acids [27]. The frequency of the asymmetric stretching band was shifted to higher frequency values in imatinib resistant cells. In addition, the changes in the intensities of the bands at 1239 and 970 cm^{-1} for the imatinib resistant cells indicate structural changes in nuclear morphology, organization, and architecture such as alterations in the nuclear/cytoplasmic ratio, hyperchromacity, chromatin aggregation and changes in DNA condensation between imatinib sensitive and resistant K562 cells. Multidrug resistance was linked to specific nuclear morphological changes acquired in the process of selection by cytotoxic drugs rather than P-gp overexpression or changes in the expression level of topoisomerase II beta [39,40].

The intensity ratio of the 1086 cm^{-1} band is due to symmetric phosphate stretching of nucleic acids and the Amide II band at 1545 cm^{-1} is used to estimate DNA/protein ratio in the cellular systems investigated [41]. In this study, the intensity ratio of 1080 cm^{-1} and Amide II bands decreased by 7.21% in K562/IMA-3 cells indicating a small decrease in the DNA over protein amount. This ratio was observed to increase in differentiated and apoptotic cells [38] and in chronic lymphatic leukemia cells during cellular differentiation [42].

The intensity ratio of the 1030 cm^{-1} and 1086 cm^{-1} bands indicates glucose/phosphate ratio as a reliable measure for metabolic turnover of the cells. The glucose/phosphate ratio was found to decrease by 12.90% in K562/IMA-3 cells. The phosphate level was higher for normal cells than for H-ras transfected malignant cells in earlier studies. Similarly, the intensity ratio of 1030 cm^{-1} and 2926 cm^{-1} bands was found to decrease by 22.03% in K562/IMA-3 cells. This ratio is indicative of the ratio of glucose/phospholipids and is a measure of de novo synthesis of phospholipids at the expense of free glucose in the cell and was found to be larger for normal cells as compared to those transformed by H-ras [43]. Decreases in both the ratios indicate an increase in the total amount of phosphate compounds in the imatinib resistant cancer cells. In cancer cell formation, the phospholipid molecules and their metabolites are believed to participate in the oncogene-induced transformation processes [44] and protein phosphorylation is known to be fostered [45]. These results also agree with the increase in the intensity of the shoulder around 1170 cm^{-1} in the imatinib resistant cancer cells indicating protein phosphorylation [46]. Gazi et al. suggested that the intensity ratio of the 1030 cm^{-1} and 1086 cm^{-1} bands could be interpreted as glycogen-to-phosphate ratio and proposed as a marker for cancer to distinguish benign and malignant prostate cancer and they concluded that the ratio decreased in malignant tissue [47].

The intensity ratio of the 1121 cm^{-1} and 1020 cm^{-1} bands was observed to increase (19.78%) in K562/IMA-3 cells. This ratio is indicative of cellular RNA/DNA ratio and is found to increase from normal to malignant cells [43]. This ratio was found to increase similar to malignant transformation. The increase in the RNA content with respect to the DNA content indicates higher necessity of transcription to deal with the toxic drug effects. Similarly, the intensity ratio of the 1121 cm^{-1} and Amide II bands decreased by 4.03% in K562/IMA-3 cells. This ratio is indicative of the transcriptional and protein expression status of the imatinib resistant cancer cells. The results indicate that the protein expression status of the K562/IMA-3 cells increases.

Different mechanisms cause drug resistance in different cancer types. In addition, a number of different drugs are used in cancer therapy many of which have been known to induce drug resistance. Hence, comprehensive molecular and spectroscopic studies should be carried out to make general conclusions about the onset and progress of resistance behavior of cancer cells against these drugs.

The results of the present study indicate that the induction of imatinib resistance in K562 cells caused alterations in cellular structure. The content of glycogen was found to decrease in the K562/IMA-3 cells. The amount of unsaturated lipids increased in the imatinib resistant cells indicating lipid peroxidation. In addition, lipid membrane order was found to increase in the K562/IMA-3 cells. Imatinib resistance caused changes in the lipid/protein ratio in the imatinib resistant cancer cells indicating possible changes in neutral lipid and lipid droplet metabolism as well as phospholipid metabolism which affect cell membrane structure. The relative content of proteins with respect to nucleic acids indicates higher transcription and protein expression and

structural/organizational changes in the nucleus as revealed by frequency changes in the nucleic acid bands. Changes in the amide bands revealed changes in the proteome of the resistant cells. The antiparallel beta sheet structure increased, however the other secondary structural elements decreased in the resistant cells. The results of the present study also revealed that FT-IR spectroscopy has the potential to be used as an analytical method of detecting and monitoring macromolecular structural and functional changes in drug resistant CML.

Disclosure of interest

The authors declare that they have no conflicts of interest concerning this article.

Acknowledgements

We thank the staff of the Biotechnology and Bioengineering Center of İzmir Institute of Technology for their help and technical support. We thank the Department of Chemistry for allowing us to use the FT-IR device.

References

[1] Druker BJ. STI571 (Gleevec) as a paradigm for cancer therapy. Trends Mol Med 2002;8:S14–8.
[2] Koca E, Haznedaroglu IC. Imatinib mesylate and the management of chronic myeloid leukemia (CML). Turk J Haematol 2005;4:161–72.
[3] Baran Y, Ural AU, Gunduz U. Mechanisms of cellular resistance to imatinib in human chronic myeloid leukemia cells. Hematology 2007;12:497–503.
[4] Baran Y, Salas A, Senkal CE, Gunduz U, Bielawski J, Obeid LM, et al. Alterations of ceramide/sphingosine 1-phosphate rheostat involved in the regulation of resistance to imatinib-induced apoptosis in K562 human chronic myeloid leukemia cells. J Biol Chem 2007;282:10922–34.
[5] Hochhaus A, La RP, Muller MC, Ernst T, Cross NC. Impact of BCR-ABL mutations on patients with chronic myeloid leukemia. Cell Cycle 2011;10:250–60.
[6] Eechoute K, Sparreboom A, Burger H, Franke RM, Schiavon G, Verweij J, et al. Drug transporters and imatinib treatment: implications for clinical practice. Clin Cancer Res 2011;17:406–15.
[7] Dogan A, Ergen K, Budak F, Severcan F. Evaluation of disseminated candidiasis on an experimental animal model: a fourier transform infrared study. Appl Spectrosc 2007;61:199–203.
[8] Cakmak G, Togan I, Severcan F. 17Beta-estradiol induced compositional, structural and functional changes in rainbow trout liver, revealed by FT-IR spectroscopy: a comparative study with nonylphenol. Aquat Toxicol 2006;77:53–63.
[9] Toyran N, Zorlu F, Severcan F. Effect of stereotactic radiosurgery on lipids and proteins of normal and hypoperfused rat brain homogenates: a Fourier transform infrared spectroscopy study. Int J Radiat Biol 2005;81:911–8.
[10] Yano K, Ohoshima S, Gotou Y, Kumaido K, Moriguchi T, Katayama H. Direct measurement of human lung cancerous and noncancerous tissues by fourier transform infrared microscopy: can an infrared microscope be used as a clinical tool? Anal Biochem 2000;287:218–25.
[11] Lewis PD, Lewis KE, Ghosal R, Bayliss S, Lloyd AJ, Wills J, et al. Evaluation of FTIR spectroscopy as a diagnostic tool for lung cancer using sputum. BMC Cancer 2010;10:640.
[12] Krishna CM, Kegelaer G, Adt I, Rubin S, Kartha VB, Manfait M, et al. Combined Fourier transform infrared and Raman spectroscopic approach for identification of multidrug resistance phenotype in cancer cell lines. Biopolymers 2006;82:462–70.
[13] Le Gal JM, Morjani H, Manfait M. Ultrastructural appraisal of the multidrug resistance in K562 and LR73 cell lines from Fourier transform infrared spectroscopy. Cancer Res 1993;53:3681–6.
[14] Ceylan C, Camgoz A, Baran Y. Macromolecular changes in nilotinib resistant K562 cells; an in vitro study by Fourier transform infrared spectroscopy. Technol Cancer Res Treat 2012;11:333–44.
[15] Ekiz HA, Can G, Gunduz U, Baran Y. Nilotinib significantly induces apoptosis in imatinib-resistant K562 cells with wild-type BCR-ABL, as effectively as in parental sensitive counterparts. Hematology 2010;15:33–8.
[16] Melin AM, Perromat A, Deleris G. Pharmacologic application of fourier transform IR spectroscopy: in vivo toxicity of carbon tetrachloride on rat liver. Biopolymers 2000;57:160–8.
[17] Severcan F, Toyran N, Kaptan N, Turan B. Fourier transform infrared study of the effect of diabetes on rat liver and heart tissues in the CH region. Talanta 2000;53:55–9.
[18] Jamin N, Dumas P, Moncuit J, Fridman WH, Teillaud JL, Carr GL, et al. Highly resolved chemical imaging of living cells by using synchrotron infrared microspectrometry. Proc Natl Acad Sci U S A 1998;95:4837–40.
[19] Dovbeshko GI, Gridina NY, Kruglova EB, Pashchuk OP. FTIR spectroscopy studies of nucleic acid damage. Talanta 2000;53:233–46.
[20] Lyman DJ, Murray-Wijelath J. Vascular graft healing: I. FTIR analysis of an implant model for studying the healing of a vascular graft. J Biomed Mater Res 1999;48:172–86.
[21] Nara M, Okazaki M, Kagi H. Infrared study of human serum very-low-density and low-density lipoproteins. Implication of esterified lipid C═O stretching bands for characterizing lipoproteins. Chem Phys Lipids 2002;117:1–6.
[22] Voortman G, Gerrits J, Altavilla M, Henning M, van BL, Hessels J. Quantitative determination of faecal fatty acids and triglycerides by Fourier transform infrared analysis with a sodium chloride transmission flow cell. Clin Chem Lab Med 2002;40:795–8.
[23] Manoharan R, Baraga JJ, Rava RP, Dasari RR, Fitzmaurice M, Feld MS. Biochemical analysis and mapping of atherosclerotic human artery using FT-IR microspectroscopy. Atherosclerosis 1993;103:181–93.
[24] Jackson M, Ramjiawan B, Hewko M, Mantsch HH. Infrared microscopic functional group mapping and spectral clustering analysis of hypercholesterolemic rabbit liver. Cell Mol Biol (Noisy-le-grand) 1998;44:89–98.
[25] Wang JJ, Chi CW, Lin SY, Chern YT. Conformational changes in gastric carcinoma cell membrane protein correlated to cell viability after treatment with adamantyl maleimide. Anticancer Res 1997;17:3473–7.
[26] Wong PT, Wong RK, Caputo TA, Godwin TA, Rigas B. Infrared spectroscopy of exfoliated human cervical cells: evidence of extensive structural changes during carcinogenesis. Proc Natl Acad Sci U S A 1991;88:10988–92.
[27] Chiriboga L, Xie P, Vigorita V, Zarou D, Zakim D, Diem M. Infrared spectroscopy of human tissue. II. A comparative study of spectra of biopsies of cervical squamous epithelium and of exfoliated cervical cells. Biospectroscopy 1998;4:55–9.
[28] Ci YX, Gao TY, Feng J, Guo JQ. Fourier transform infrared spectroscopic characterization of human breast tissue: implications for breast cancer diagnosis. Appl Spectrosc 1999;53:312–5.
[29] Mahon FX, Hayette S, Lagarde V, Belloc F, Turcq B, Nicolini F, et al. Evidence that resistance to nilotinib may be due to BCR-ABL, Pgp, or Src kinase overexpression. Cancer Res 2008;68:9809–16.
[30] Kim HH, Kim T, Kim E, Park JK, Park SJ, Joo H. The mitochondrial Warburg effect: a cancer enigma. Interdisciplinary Bio Central 2009;1:1–7.
[31] Severcan F, Gorgulu G, Gorgulu ST, Guray T. Rapid monitoring of diabetes-induced lipid peroxidation by Fourier transform infrared spectroscopy: evidence from rat liver microsomal membranes. Anal Biochem 2005;339:36–40.
[32] Takahashi H, French SW, Wong PT. Alterations in hepatic lipids and proteins by chronic ethanol intake: a high-pressure Fourier transform infrared spectroscopic study on alcoholic liver disease in the rat. Alcohol Clin Exp Res 1991;15:219–23.
[33] Schuldes H, Dolderer JH, Zimmer G, Knobloch J, Bickeboller R, Jonas D, et al. Reversal of multidrug resistance and increase in plasma membrane fluidity in CHO cells with R-verapamil and bile salts. Eur J Cancer 2001;37:660–7.
[34] Tsvetkova NM, Horvath I, Torok Z, Wolkers WF, Balogi Z, Shigapova N, et al. Small heat-shock proteins regulate membrane lipid polymorphism. Proc Natl Acad Sci U S A 2002;99:13504–9.
[35] Lavie Y, Fiucci G, Czarny M, Liscovitch M. Changes in membrane microdomains and caveolae constituents in multidrug-resistant cancer cells. Lipids 1999;34:S57–63.
[36] Mannechez A, Reungpatthanaphong P, de Certaines JD, Leray G, Le ML. Proton NMR visible mobile lipid signals in sensitive and multidrug-resistant K562 cells are modulated by rafts. Cancer Cell Int 2005;5:2.
[37] Jackson M, Mansfield JR, Dolenko B, Somorjai RL, Mantsch HH, Watson PH. Classification of breast tumors by grade and steroid receptor status using pattern recognition analysis of infrared spectra. Cancer Detect Prev 1999;23:245–53.
[38] Zhou J, Wang Z, Sun S, Liu M, Zhang H. A rapid method for detecting conformational changes during differentiation and apoptosis of HL60 cells by Fourier-transform infrared spectroscopy. Biotechnol Appl Biochem 2001;33:127–32.
[39] Dufer J, Millot-Broglio C, Oum'Hamed Z, Liautaud-Roger F, Joly P, Desplaces A, et al. Nuclear DNA content and chromatin texture in multidrug-resistant human leukemic cell lines. Int J Cancer 1995;60:108–14.
[40] McNamara S, Miller Jr WH. Expanding the use of retinoids in acute myeloid leukemia: spotlight on bexarotene. Clin Cancer Res 2008;14:5311–3.
[41] Mourant JR, Yamada YR, Carpenter S, Dominique LR, Freyer JP. FTIR spectroscopy demonstrates biochemical differences in mammalian cell cultures at different growth stages. Biophys J 2003;85:1938–47.
[42] Benedetti E, Vergamini P, Spremolla G. Ft-Ir analysis of single human normal and leukemic lymphocytes. Mikrochim Acta 1998;1:139–41.
[43] Ramesh J, Salman A, Hammody Z, Cohen B, Gopas J, Grossman N, et al. Application of FTIR microscopy for the characterization of malignancy: H-ras transfected murine fibroblasts as an example. J Biochem Biophys Methods 2001;50:33–42.
[44] Dobrzyńska I, Szachowicz-Petelska B, Sulkowski S, Figaszewski Z. Changes in electric charge and phospholipids composition in human colorectal cancer cells. Mol Cell Biochem 2005;276:113–9.
[45] Fine RL, Patel J, Chabner BA. Phorbol esters induce multidrug resistance in human breast cancer cells. Proc Nat Acad Sci U S A 1998;85:582–6.
[46] Yazdi HM, Bertrand MA, Wong PT. Detecting structural changes at the molecular level with Fourier transform infrared spectroscopy. A potential tool for prescreening preinvasive lesions of the cervix. Acta Cytol 1996;40:664–8.
[47] Gazi E, Dwyer J, Gardner P, Ghanbari-Siahkali A, Wade AP, Miyan J, et al. Applications of Fourier transform infrared microspectroscopy in studies of benign prostate and prostate cancer. A pilot study. J Pathol 2003;201:99–108.